ResearchGate

See discussions, stats, and author profiles for this publication at: https://www.researchgate.net/publication/6761457

Vibrational spectra and structures of H2O−NO, HDO−NO, and D2O−NO complexes. An IR matrix isolation and DFT study

ARTICLE *in* THE JOURNAL OF PHYSICAL CHEMISTRY A · NOVEMBER 2006

Impact Factor: 2.69 · DOI: 10.1021/jp0625614 · Source: PubMed

CITATIONS
14

READS
70

4 AUTHORS, INCLUDING:

Nadia Dozova
Ecole Normale Supérieure de Paris
10 PUBLICATIONS **69** CITATIONS
SEE PROFILE

M. Esmail Alikhani
Pierre and Marie Curie University - Paris 6
107 PUBLICATIONS **1,264** CITATIONS
SEE PROFILE

Nelly Lacome
Pierre and Marie Curie University - Paris 6
96 PUBLICATIONS **3,190** CITATIONS
SEE PROFILE

Available from: M. Esmail Alikhani
Retrieved on: 23 January 2016

Vibrational Spectra and Structures of H_2O-NO, $HDO-NO$, and D_2O-NO Complexes. An IR Matrix Isolation and DFT Study

Nadia Dozova, Lahouari Krim,* M. Esmaïl Alikhani, and Nelly Lacome

Université Pierre et Marie Curie-Paris6; CNRS, LADIR UMR 7075, Boîte 49, 4 Place Jussieu, 75252 Paris, Cedex 05, France

Received: April 26, 2006; In Final Form: July 19, 2006

The IR spectra of H_2O + NO, HDO + NO, and D_2O + NO, isolated in solid neon at low temperature have been investigated. Concentration effects and detailed vibrational analysis of deuterated and partially deuterated species allowed identification of three 1:1 HDO−NO species, two 1:1 D_2O-NO species, and only one 1:1 H_2O-NO complex. From comparison between the experimental spectra and the results of DFT calculations, it appeared that two different types of weakly bound complexes between water and nitric oxide can be formed in a neon matrix. The first species is a 1:1 complex where bonding occurs between water hydrogen and nitric oxide nitrogen, in which OH−N and OD−N intermolecular bonds are engaged. For this complex only DOD−NO, HOD−NO, and DOH−NO isotopic species have been experimentally detected and no IR bands of HOH−NO were observed. This result could be explained by the fact that the dissociation energy of HOH−NO is lower than those of DOD−NO, HOD−NO and DOH−NO. For the second detected 1:1 H_2O-NO complex and its isotopic variants, the H_2O-NO potential surface was explored systematically at the B3LYP level, but no stable species corresponding to the complex could be calculated. The structure of the second observed 1:1 H_2O-NO complex results from columbic attractions between water and nitric oxide and could be stabilized only in matrix, probably by interaction between NO, water and $(Ne)_n$.

Introduction

Studies of weakly bonded molecular complexes formed between water and atmospheric molecules such as N_2, O_2, CO, and NO can give important information on molecular interactions in atmospheric and astrophysical chemistry. Van der Waals and hydrogen bonded molecular complexes have motivated both theoretical and experimental studies[1]. Sandler et al.[1] analyzed a weakly bonded cluster of water with nitrogen which combined ab initio calculations of the potential energy surface with diffusion Monte Carlo calculations of the vibrational ground state for different H_2O-N_2 isotopic species. Coussan et al.[2] investigated the infrared spectra of $H_2O + N_2$ reaction in argon matrix. They identified several $(H_2O)_m(N_2)_n$ species such as H_2O-N_2 and $(H_2O)_2-N_2$. The structural properties of these two complexes are discussed on the basis of ab initio calculations, carried out within the framework of the density functional theory (DFT). Hirabayashi et al.[3] reported IR absorption bands of $H_2O-(N_2)_n$ complexes isolated in solid argon. Kjaegaard et al.[4] calculated the OH-stretching vibrational transitions in the water−nitrogen and water−oxygen complexes. They also discussed the possible effect of H_2O-N_2 and H_2O-O_2 on the atmospheric absorption of solar radiation. Cooper et al.[5] provided, only recently, evidence for the existence of the H_2O-O_2 complex in argon matrix. Theoretical studies of the H_2O-O_2 complex have been carried out, but the complex has not previously been experimentally identified. This identification may possibly help astronomers identifying O_2 in icy satellite surfaces and interstellar grains. Surprisingly H_2O-NO was the object of only two theoretical papers[6−7] and one experimental study.[8] The H_2O-NO complex isolated in nitrogen matrix was examined by infrared spectroscopy[8] in 1973. The study was very poor with no conclusive identification of the isolated species. Spectra of H_2O + NO showed some absorption peaks which were assigned to complexes, but no information, such as what peaks belong to what kind of complex, were given. In 1998, Givan et al.[9] assigned two absorption peaks (close to the ν_{NO} and ν_3 of H_2O) to the 1:1 H_2O-NO species, in an infrared study of molecular complexes of sulfuric acid with N_2 and NO trapped in solid argon. Theoretical calculations of the energetic properties of H_2O-NO complex have been published by D. W. Ball using the G2 method[6] and by Myszkiewicz et al.[7] using the unrestricted MP2, MP4 and CCSD(T) methods. Both studies showed that the most stable geometry for the H_2O-NO complex is the one where the bonding occurs between one water hydrogen atom and the NO nitrogen atom. The calculations showed that H_2O-NO is a very weak complex with D_e of about 4.5 kJ/mol. The bonding between the H atom of water and the O atom of NO resulted in a less stable structure. Unfortunately the frequencies for the different structures of the complex were not given in the literature. Therefore, the study of molecular complexes involving NO and H_2O is still a challenging problem.

In the present study, the structure of different isotopic species of H_2O-NO complexes were investigated by neon matrix-isolation combined with infrared absorption spectroscopy. Detailed vibrational assignments were made from the observed spectra of H_2O + NO system. Using DFT calculations, geometrical and vibrational properties of the complex have been estimated.

Experimental Technique

H_2O + NO samples were prepared by co-condensing $NO/H_2O/Ne$ mixtures onto a cryogenic metal mirror maintained at 5 K. Molar ratios (X/Ne: X = NO or H_2O) ranged from

* To whom correspondence should be addressed. E-mail: krim@ccr.jussieu.fr.

10.1021/jp0625614 CCC: $33.50 © 2006 American Chemical Society
Published on Web 09/26/2006

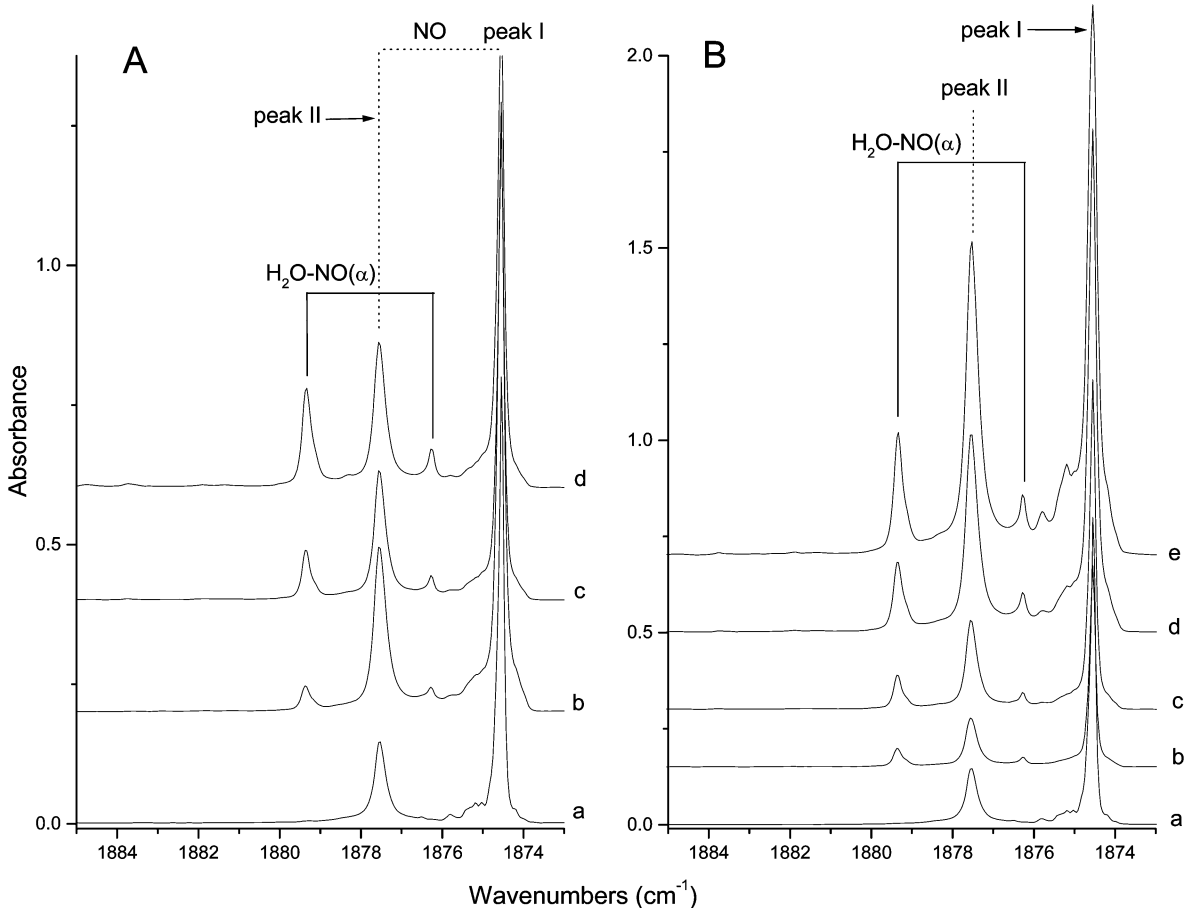

Figure 1. (A) Effects of H_2O concentration on H_2O-NO bands in the NO stretching mode (ν_{NO}) region: (a) NO/Ne = 5/10000; (b) NO/H_2O/Ne = 5/0.5/10000; (c) NO/H_2O/Ne = 5/1/10000; (d) NO/H_2O/Ne = 5/5/10000. (B) Effects of NO concentration on H_2O-NO bands in the NO stretching mode (ν_{NO}) region: (a) NO/Ne = 5/10000; (b) NO/H_2O/Ne = 5/1/10000; (c) NO/H_2O/Ne = 10/1/10000; (d) NO/H_2O/Ne = 20/1/10000; (e) NO/H_2O/Ne = 40/1/10000.

0.001% up to 1%. The experimental method and setup have been previously described into details.[10] We shall recall only the main points. Deposition times were around 60 mn. Neon and NO gases were obtained from "L'Air liquide" with purities of 99.9995% and 99.9%, respectively. D-isotopic water (Eurisotop 99.90%) as well as natural water was degassed in a vacuum line. The purity of samples was confirmed spectroscopically.

Infrared spectra of the resulting samples were recorded in the transmission-reflection mode between 4500 and 500 cm^{-1} using a Bruker 120 FTIR spectrometer equipped with a KBr/Ge beam splitter and a liquid N_2-cooled narrow band HgCdTe photoconductor. A resolution of 0.1 cm^{-1} was used. Bare mirror backgrounds, recorded from 4500 to 500 cm^{-1} prior to sample deposition, were used as references in processing the sample spectra. Absorption spectra in the mid-infrared were collected on samples through a KBr window mounted on a rotatable flange separating the interferometer vacuum (10^{-3} mbar) from that of the cryostatic cell (10^{-7} mbar). The spectra were subsequently subjected to baseline correction to compensate for infrared light scattering and interference patterns. All spectra were recorded at 5 K.

The samples could be irradiated using a 200 W mercury−xenon high-pressure arc lamp and either interference narrow (5 nm fwhm) or broad band filters in order to find if some photoprocesses could be initiated by UV−visible or near-infrared light. Next, or after sample annealing up to 12 K in several steps, infrared spectra of the samples were recorded again between 4500 and 500 cm^{-1} as outlined above.

Experimental Results

H_2O—NO in Ne Matrix. Upon co-deposition of a mixture H_2O/NO/Ne new bands appear in the NO stretching region and in the vibrational mode regions of water, in addition to those attributed to unreacted NO, H_2O, and $(H_2O)_2$ species. These bands are assigned to complexes between H_2O and NO. All experiments were performed with weak concentrations of NO and H_2O molecules in order to form the 1:1 H_2O-NO complex and to control its evolution by changing the matrix temperature.

NO Stretching Region. The spectrum of NO in a neon matrix has been extensively studied.[11] In our experiments NO/Ne was deposited at 5 K. The stretching of the NO monomer consists of two bands: peak I (intense) at 1874.6 cm^{-1} and peak II (weaker) at 1877.5 cm^{-1} which have been assigned to NO in two different substitutional sites of the neon matrix (Figure 1a). Upon annealing, other bands corresponding to the NO monomer appear in this region. They have been assigned to monomers close together, but hindered by the matrix cage to form the NO dimer. Other broad absorptions belonging to *cis*-$(NO)_2$ are present in the spectra at 1865 cm^{-1} (symmetric NO stretching) and 1779.6 cm^{-1} (antisymmetric NO stretching).

The spectrum of NO + H_2O samples shows two new peaks situated on the blue side of peak I of the NO monomer, at 1876.3 and 1879.4 cm^{-1} (Figure 1). The intensities of both peaks depend linearly upon the concentration of H_2O (Figure 1A) and NO (Figure 1B). The shifts between these bands and peaks I

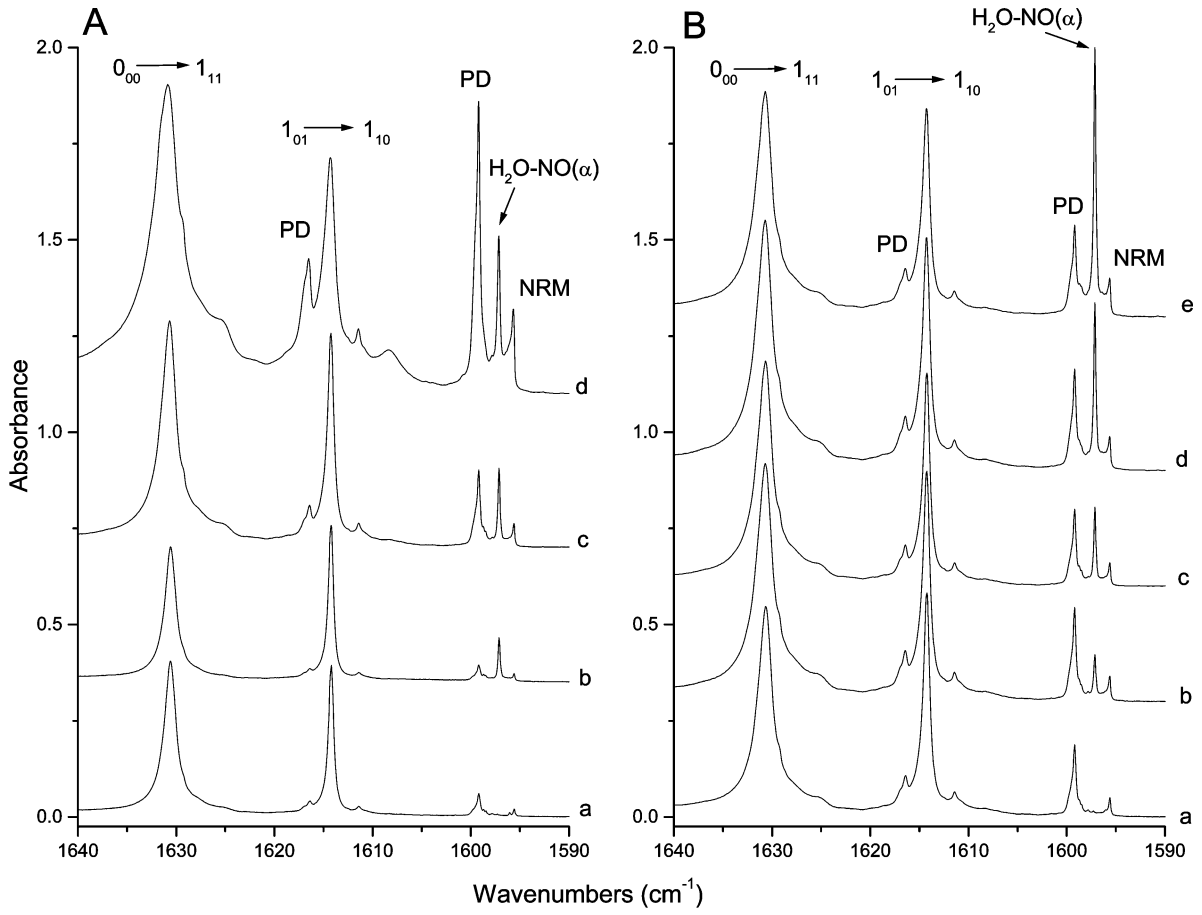

Figure 2. (A) Effects of H_2O concentration on H_2O−NO bands in the HOH bending mode (ν_2) region: (a) H_2O/Ne = 0.5/10000; (b) NO/H_2O/Ne = 5/0.5/10000; (c) NO/H_2O/Ne = 5/1/10000; (d) NO/H_2O/Ne = 5/5/10000. (B) Effects of NO concentration on H_2O−NO bands in the HOH bending mode (ν_2) region: (a) H_2O/Ne = 1/10000; (b) NO/H_2O/Ne = 5/1/10000; (c) NO/H_2O/Ne = 10/1/10000; (d) NO/H_2O/Ne = 20/1/10000; (e) NO/H_2O/Ne = 40/1/10000.

and II of NO monomer are equal to +1.9 and +1.7 cm^{-1}, respectively. These shifts are almost equal, and thus, the two peaks can be assigned to a H_2O−NO complex isolated in two different substitutional sites in the neon matrix. New bands with same behavior as bands at 1876.3 and 1879.4 cm^{-1} are also observed in the spectral regions of H_2O (ν_1, ν_2, ν_3).

H_2O Vibrational Regions. Water molecules isolated in a rare gas matrix have the particularity of rotating inside the matrix cage, and thus the rovibrational spectrum of water monomers can be observed.[12−16] Thus the H_2O rovibrational transitions (labeled $J''_{K''a\ K''c} \rightarrow J'_{K'a\ K'c}$) of the rotating monomer (RM) give rise to several rovibrational lines. Other water molecules are trapped in matrix sites where their rotation is strongly hindered. These nonrotating monomers (NRM) give rise to transitions close to the pure vibrational frequencies. The three vibrational fundamentals of H_2O NRM (Figures 2a and 3a) are situated at 1595.6 cm^{-1} (HOH bending ν_2), at 3665.5 cm^{-1} (symmetric stretching ν_1) and 3761.1 cm^{-1} (antisymmetric stretching ν_3).[17]

Spectra of H_2O + NO samples show new bands in the three vibrational regions of H_2O. A new peak appears in the HOH bending (ν_2) region at 1597.1 cm^{-1} (Figure 2). Figure 3A shows another band that appears at 3660.9 cm^{-1} in the ν_1 region of the proton acceptor (PA) of the water dimer[17] situated at 3660.5 cm^{-1}. In the antisymmetric OH stretching region a new band is observed at 3771.3 cm^{-1} (Figure 3B). All these bands depend linearly upon the concentration of both NO and H_2O and have been attributed to the H_2O−NO complex.

Figures 1−3 show the spectra of NO + H_2O samples, indicating that the bands of H_2O−NO complex (and those of H_2O and NO molecules) increase linearly with NO and H_2O concentrations. In the following, we will take the NO stretching (ν_{NO}) and symmetric OH stretching (ν_1) spectral regions as a characteristic domain of the specific vibrational modes of the H_2O−NO complex.

Matrix Temperature Effects. The annealing of the matrix allows not only the formation of the complex H_2O−NO but also the formation of complexes of greater size like $(H_2O)_2$−NO and H_2O−$(NO)_2$ because of the diffusion of NO and water molecules. Figure 4A shows the evolution of the bands of the complex in the NO stretching mode region. Upon annealing to 9 K, H_2O and NO molecules diffuse in the matrix in order to form the complex H_2O−NO (the intensity of band at 1876.3 cm^{-1} increases) and $(H_2O)_2$−NO (species observed at 1883.8 cm^{-1}). NO molecules trapped in site II do not diffuse through the matrix: the intensities of the peaks at 1879.4 cm^{-1} (NO−H_2O traped in site II) and 1877.5 cm^{-1} (peak II of NO monomer) remain constant. Upon annealing to 11 K, the band of H_2O−NO trapped in site I decreases, while the band of H_2O−NO in site II remains constant. At 11 K, the global concentration of H_2O−NO in the matrix decreases in order to form higher stoechiometry complexes such as $(H_2O)_2$−NO species (band observed at 1883.8 cm^{-1}). At 12 K, all the bands of H_2O−NO complex (and those of NO monomer) have disappeared. The intensity of the band of $(H_2O)_2$−NO (1883.8 cm^{-1}) remains constant, while other bands (assigned to $(H_2O)_n$−NO

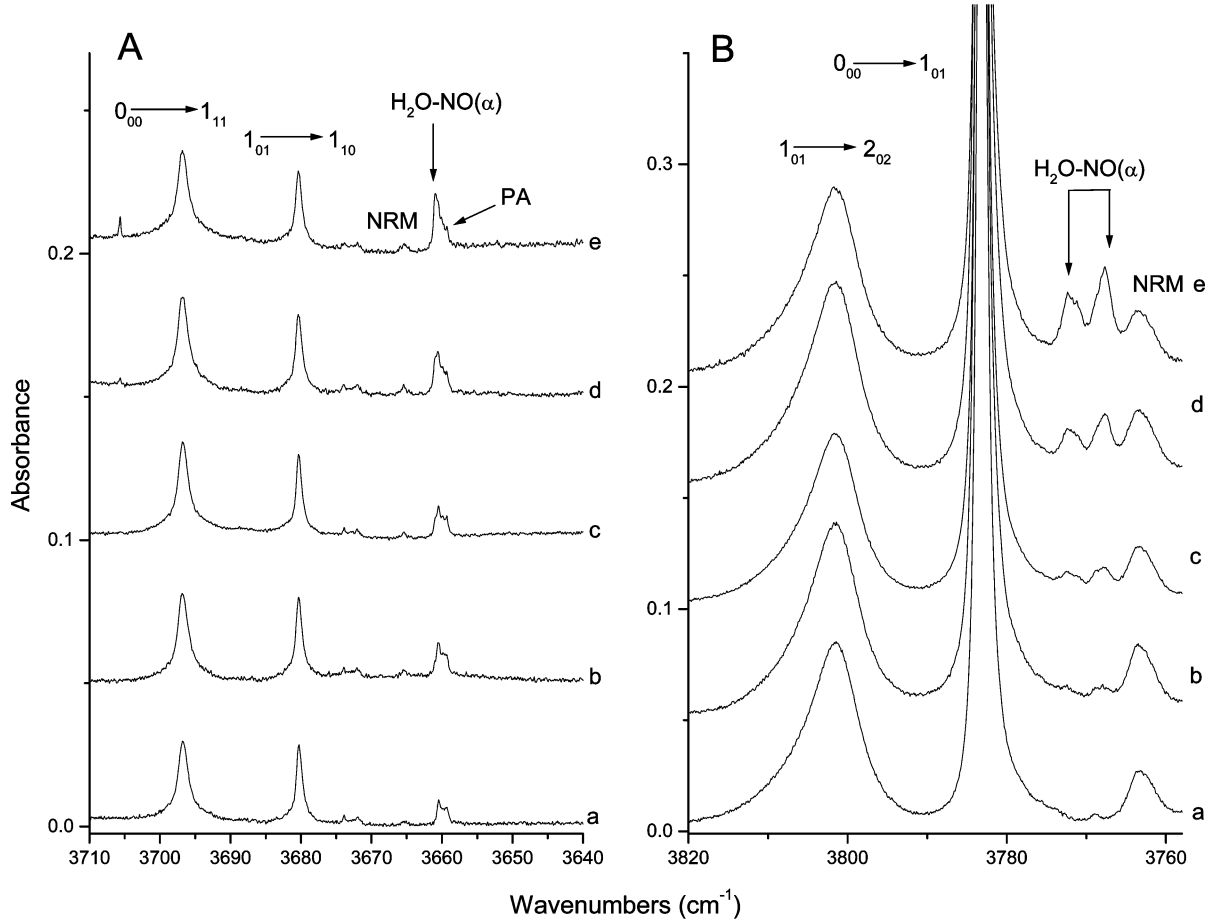

Figure 3. Effects of NO concentration on H_2O-NO bands in the symmetric OH stretching mode (ν_1) (A) and antisymmetric OH stretching mode (ν_3) (B) regions: (a) H_2O/Ne = 1/10000; (b) NO/H_2O/Ne = 5/1/10000; (c) NO/H_2O/Ne = 10/1/10000; (d) NO/H_2O/Ne = 20/1/10000; (e) NO/H_2O/Ne = 40/1/10000.

($n \geq 3$)) increase at 1881.3 and 1880.7 cm^{-1}. This fact allows the differentiation between 1:1, 1:2 and 1:n ($n \geq 3$) $(H_2O)_n-NO$ complexes. The characteristic bands of the H_2O-NO complex increase upon annealing to 9 K, decrease upon annealing to 11 K, and fully disappear upon annealing to 12 K. The bands of $(H_2O)_2-NO$ increase between 5 and 11 K and remain constant at 12 K while aggregates such $(H_2O)_n-NO$ appear after annealing upon 12 K. The concentration of H_2O-NO complex trapped in the matrix is maximum at 9 K.

Figure 4B shows the effect of annealing upon the bands in the OH symmetric stretching region. Upon annealing to 12 K, the band of H_2O-NO (3660.9 cm^{-1}) disappears while intensities of bands attributed to higher stoechiometry complexes increase.

Table 1 shows the frequency modes of NO, H_2O, and H_2O-NO and the frequency shifts with respect to the monomeric moieties.

D_2O—NO in Ne Matrix. *NO Stretching Region.* Figure 5 shows the spectra of H_2O/NO/Ne and D_2O/NO/Ne after annealing to 9 K. The bands of $NO-H_2O$ at 1876.3 and 1879.4 cm^{-1} are shifted to 1876.4 and 1879.5 cm^{-1} for $NO-D_2O$ species. The band of the complex $(H_2O)_2-NO$ at 1883.8 cm^{-1} is shifted to 1884.3 cm^{-1} for the complex $(D_2O)_2-NO$. A new band appears at 1882.9 cm^{-1} in the D_2O + NO sample. The intensity of this new band increases linearly with D_2O and NO concentrations and could be assigned to a new species containing one NO and one D_2O molecule. Its behavior is similar to the behavior of the bands at 1876.4 and 1879.5 cm^{-1}, assigned to D_2O-NO isotopomer of H_2O-NO. The band of the new species D_2O-NO increase upon annealing to 9 K, decrease upon annealing to 11 K and fully disappear upon annealing to 12 K (Figure 6). No band corresponding to this new species was observed in the NO + H_2O samples.

D_2O Vibrational Regions. D_2O spectral regions are similar to those of H_2O. However, they are spectrally more compact due to the smaller rotational constant of D_2O. The NRM peak in the ν_2 D_2O spectral region is located at 1178.8 cm^{-1}. In the ν_1 and ν_3 mode regions the NRM bands are located at 2676.7 and 2785.9 cm^{-1}, respectively.[17] Figure 7 shows the region of symmetric OD stretching of D_2O/NO/Ne mixture after deposition at 5 K and annealing to 9 and 12 K.As in NO spectral region, two different bands that increase linearly with D_2O and NO concentrations are visible at 2673.8 and 2666.9 cm^{-1}. They increase upon annealing to 9 K and disappear upon annealing to 12 K and could be attributed to two D_2O-NOspecies (Figure 7). Figure 4B (at 5 and 9 K) shows the region of symmetric OH stretching of H_2O + NO sample. It is obvious that in the case of NO + H_2O only one complex H_2O-NO is observed.

The spectrum of NO + H_2O sample shows only one complex (denoted $NO-H_2O(\alpha)$) which is characterized by weak vibrational shifts with respect to the monomeric moieties. The spectrum of NO + D_2O sample shows that in addition to $D_2O-NO(\alpha)$ (characterized by weak vibrational shifts) another complex $NO-D_2O(\beta)$ is trapped in the neon matrix. $D_2O-NO(\beta)$ species behaves like $D_2O-NO(\alpha)$, with regard to water and NO concentration and matrix annealing, but with larger vibrational shifts with respect to the monomeric moieties.

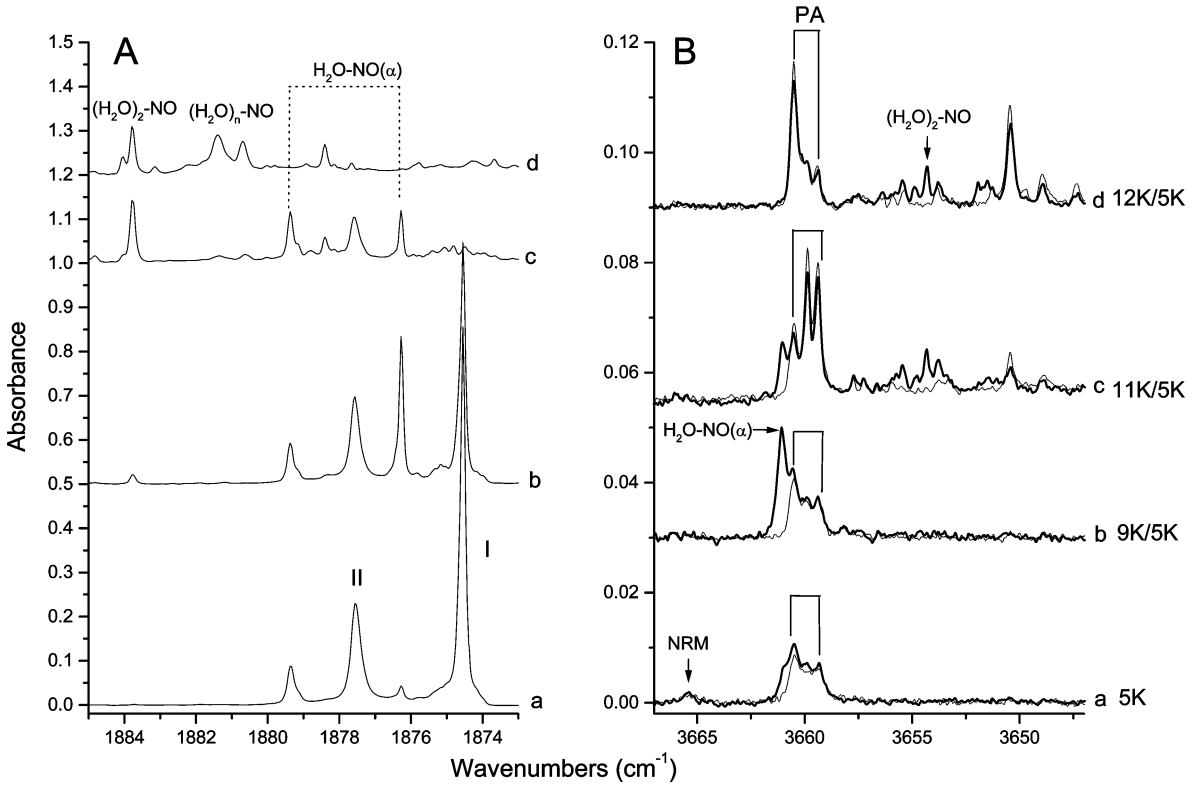

Figure 4. Annealing effects on H_2O-NO bands in the NO stretching mode (ν_{NO}) (A) and in the symmetric OH stretching mode (ν_1) (B) regions: (a) after deposition at 5 K; (b) after annealing to 9 K; (b) after annealing to 11 K; (b) after annealing to 12 K. All spectra were recorded at 5 K. Key: (−) $NO/H_2O/Ne = 10/1/10000$; (- -) $H_2O/Ne = 1/10000$.

TABLE 1: Vibrational Mode Frequencies (in cm^{-1}) of H_2O, NON, and $H_2O-NO(\alpha)$ Complex in Neon Matrix

	monomers	$H_2O-NO(\alpha)$	shift
ν_1	3665.5	3660.9	−4.6
ν_2	1595.6	1597.1	+1.5
ν_3	3761.1	3771.3	+10.2
ν_{NO} site 1	1874.6	1876.3	+1.7
site 2	1877.5	1879.4	+1.9

In the regions of DOD bending and asymmetric OD stretching, like in the region of symmetric OD stretching, bands belonging to $D_2O-NO(\alpha)$, similar to those of $H_2O-NO(\alpha)$ and characterized by weak vibrational shifts, are observed at 1179.4 and 2794.3 cm^{-1} and bands belonging to the new species $D_2O-NO(\beta)$ at 1180.4 and 2780.2 cm^{-1}.

The frequency modes of D_2O, NO, $D_2O-NO(\alpha)$, and $D_2O-NO(\beta)$ are summarized in Table 2.

HDO—NO in Ne Matrix. *NO Stretching Region.* The spectra of D_2O-NO and HDO−NO are similar, indicating the existence of HDO−NO(α) and HDO−NO(*β*). The NO stretching frequency in HDO−NO(α) is equal to the one in $D_2O-NO(\alpha)$. The NO stretching frequency in HDO−NO(*β*) is also identical to the one in $D_2O-NO(\beta)$.

HDO Vibrational Regions. HDO spectral regions are similar to those of H_2O and D_2O. In the HDO molecule, the two O−D

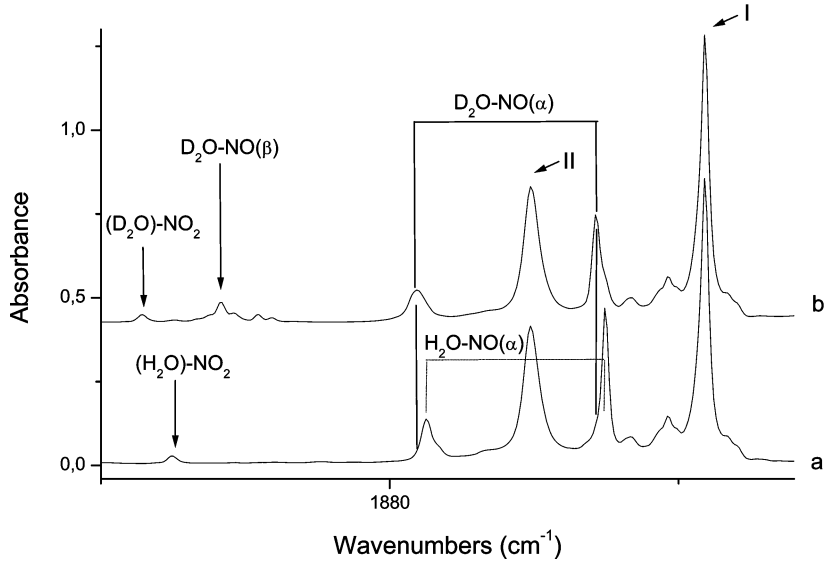

Figure 5. Spectra after annealing at 9 K of H_2O-NO and D_2O-NO bands in the NO stretching mode (ν_{NO}) region: (a) $NO/H_2O/Ne = 20/1/10000$; (b) $NO/D_2O/Ne = 20/1/10000$. Spectra recorded at 5 K.

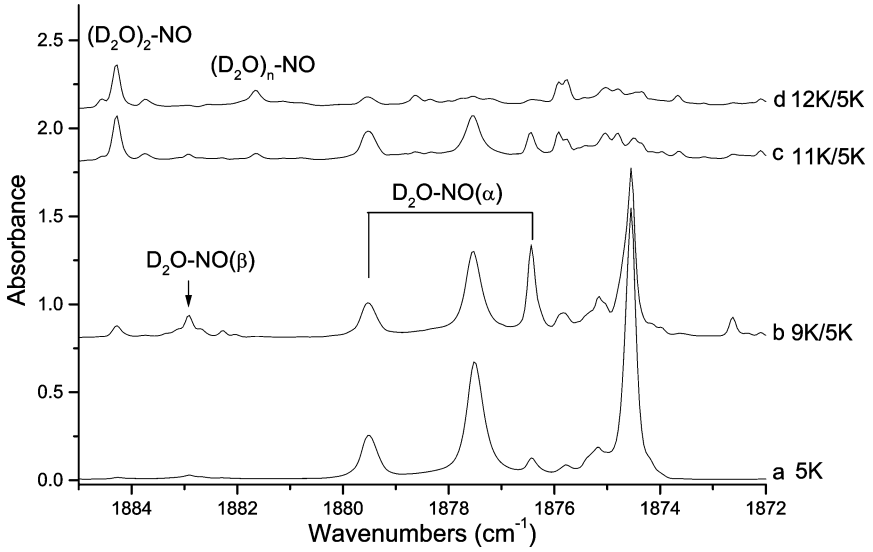

Figure 6. Annealing effects on D_2O-NO bands in the NO stretching mode (ν_{NO}) region: (a) after deposition at 5 K; (b) after annealing to 9 K; (c) after annealing to 11 K; (d) after annealing to 12 K. All spectra were recorded at 5 K. $NO/D_2O/Ne = 20/1/10000$.

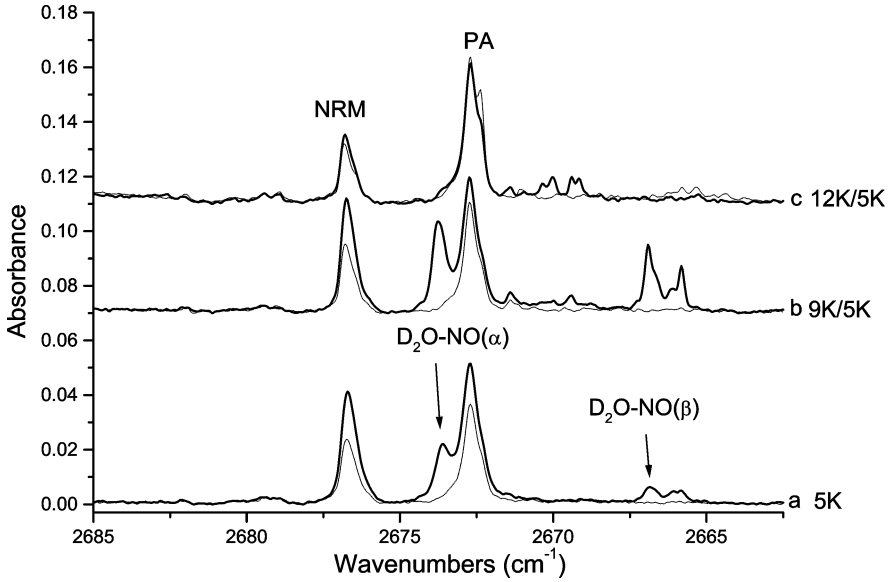

Figure 7. Annealing effects on D_2O-NO bands in the symmetric OD stretching mode (ν_1) region: (a) after deposition at 5 K; (b) after annealing to 9 K; (c) after annealing to 12 K. All spectra were recorded at 5 K. Key: (−) $NO/D_2O/Ne = 20/1/10000$; (- -) $D_2O/Ne = 1/10000$.

TABLE 2: Vibrational Mode Frequencies (in cm^{-1}) of D_2O, NO, and $D_2O-NO(\alpha$ and $\beta)$ Complexes in Neon Matrix

	monomers	$D_2O-NO(\alpha)$	shift	$D_2O-NO(\beta)$	shift
ν_1	2676.7	2673.8	−2.9	2666.9	−9.8
ν_2	1178.7	1179.4	+0.7	1180.4	+1.7
ν_3	2785.9	2794.3	+8.4	2780.2	−5.7
ν_{NO} site 1	1874.6	1876.4	+1.8	1882.9	+8.3
site 2	1877.5	1879.5	+2		

and O−H bonds are not equivalent anymore. The ν_1 corresponds to O−D stretching mode and the ν_3 corresponds to O−H stretching mode. For the NRM the HOD bending (ν_2) is situated at 1404.2 cm^{-1}, the O−D stretching (ν_1) at 2727.4 cm^{-1} and the O−H stretching (ν_3) 17 at 3706.6 cm^{-1}.

In the OD stretching region three bands at 2724.2, 2735.2, and 2709.8 cm^{-1} are observed (Figure 8). They all belong to species that contain one water and one NO molecule. Their behavior is similar to that of the bands assigned to HDO−NO-(α and β) in the NO stretching region. The weak shifted band at 2724.2 cm^{-1} from HDO monomer (NRM) allows us to assign this band to $HDO-NO(\alpha)$. (The frequency shift with respect to ν_1 in $H_2O-NO(\alpha)$ is −4.6 cm^{-1}, in $D_2O-NO(\alpha)$ is −2.9 cm^{-1} and in $HDO-NO(\alpha)$ is −3.2 cm^{-1}). Thus $NO-HDO(\alpha)$ and $D_2O-NO(\alpha)$ are the isotopomer species of $H_2O-NO(\alpha)$ complex.

With respect to the ν_{OD} band of the D_2O monomer, the band attributed to $D_2O-NO(\beta)$ species is red shifted by −9.8 cm^{-1}. In the same way, the band at 2709.8 cm^{-1} is red shifted by −17.6 cm^{-1} (with respect to the ν_{OD} band of the HOD monomer) and so this band could be assigned to the complex $HDO-NO(\beta)$ which is an isotopomer species of $D_2O-NO(\beta)$ complex. The last new band, at 2735.2 cm^{-1}, is blue shifted by 7.8 cm^{-1} (no corresponding bands is observed in the spectra of $H_2O + NO$ and $D_2O + NO$) and has been assigned to a third species $HDO-NO(\beta')$.

In the HOD bending region three bands are also observed at 1405.3, 1416.4, and 1402.8 cm^{-1}, which correspond to the three species formed by the association of NO and HOD. In the OH stretching region of HDO, bands due to the HOD monomer (RM and NRM) and to $(HOD)_2$ overlap and only two bands

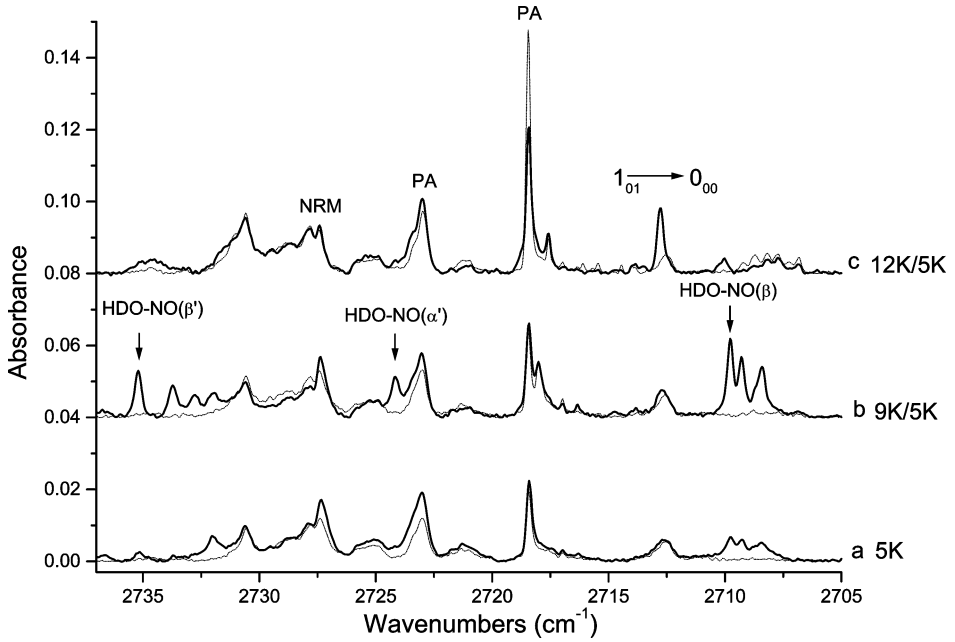

Figure 8. Annealing effects on HDO−NO bands in the OD stretching mode (ν_1) region: (a) after deposition at 5 K; (b) after annealing to 9 K; (c) after annealing to 12 K. All spectra were recorded at 5 K. Key: (−) NO/H_2O/D_2O/Ne = 20/0.5/0.5/10000; (- -) H_2O/D_2O/Ne = 0.5/0.5/10000.

TABLE 3: Vibrational Mode Frequencies (in cm^{-1}) of HDO, NO, and HDO−NO(α, *β*, and *β′*) Complexes in Neon Matrix

	monomers	HDO−NO(α)	shift	HDO−NO(*β*)	shift	HDO−NO(*β′*)	shift
ν_1	2727.4	2724.2	−3.2	2709.8	−17.6	2735.2	7.8
ν_2	1404.2	1405.3	+1.1	1402.8	−1.4	1416.4	12.2
ν_3	3706.6	3716.2	+9.6	3712.2	5.6	−	−
ν_{NO} site 1	1874.6	1876.4	+1.8	+1882.9	+8.3	1882.9	+8.3
site 2	1877.5	1879.5	+2				

characteristic of the species 1:1 HDO−NO were observed at 3716.2 and 3712.2 cm^{-1}.

Isolation of NO + H_2O in neon matrix results in the formation of the complex H_2O−NO(α), characterized by small vibrational shifts. Samples with NO + D_2O show the existence of two different 1:1 species: the complex D_2O−NO(α) which is an isotopomer of H_2O−NO(α) and the complex D_2O−NO(*β*). Spectra of HDO + NO show the existence of three different 1:1 species in the neon matrix. HDO−NO(α), which is an isotopomer of H_2O−NO(α) and D_2O−NO(α), and the two complexes HDO−NO(*β*) and HDO−NO(*β′*) that have the same NO stretching frequency as D_2O−NO(*β*).

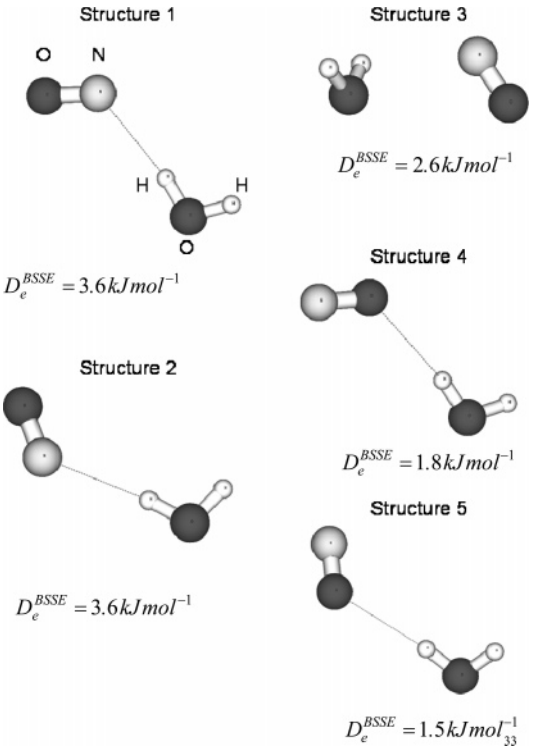

Figure 9. The five different structures studied for the H_2O−NO complex.

TABLE 4: Calculated Geometric Parameters[a] and Stability of the Five Structures of the H_2O−NO Complex

	monomers	structure 1	structure 2	structure 3	structure 4	structure 5
D_e		4.5	4.0	3.5	2.5	2.3
D_e^{BSSE}		3.6	3.6	2.6	1.8	1.5
r_{OH}[b]	0.961	0.963	0.963	0.961	0.962	0.962
r_{OH}	0.961	0.961	0.961	0.961	0.961	0.961
$\angle_{HOH}$	105.1	105.2	105.3	105.0	105.2	105.2
r_{NO}	1.147	1.145	1.146	1.147	1.148	1.148

r_{H---N}	r_{H---N}	r_{O---N}	r_{H---O}	r_{H---O}
2.341	2.356	2.994	2.399	2.376

[a] Distances in Å, angles in degrees, D_e and D_e^{BSSE} in kJ mol^{-1}. [b] OH bond perturbed by the presence of NO.

TABLE 5: Comparison of the Calculated Frequency Shifts (cm^{-1}) for the Five Structures of H_2O−NO with the Matrix Data

	structure 1 calcd	structure 2 calcd	structure 3 calcd	structure 4 calcd	structure 5 calcd	H_2O−NO(α) obsd
$\Delta\nu_1$	−25.4	−21.4	−3.0	−6.8	−6.0	−4.6
$\Delta\nu_2$	3.7	2.5	1.9	1.8	0.1	+1.5
$\Delta\nu_3$	−17.7	−15.8	−4.7	−7.5	−6.7	+10.2
$\Delta\nu_{NO}$	12.1	9.2	−2.3	−6.8	−5.6	+1.7

TABLE 6: Comparison of the Calculated Frequency Shifts (cm^{-1}) for the Five Structures of D_2O-NO with the Matrix Data

	structure 1 calcd	structure 2 calcd	structure 3 calcd	structure 4 calcd	structure 5 calcd	$D_2O-NO(\alpha)$ obsd	$D_2O-NO(\beta)$ obsd
$\Delta\nu_1$	−16.6	−14.2	−2.0	−4.7	−4.2	−2.9	−9.8
$\Delta\nu_2$	1.9	1.3	1.3	0.9	−0.2	0.7	1.7
$\Delta\nu_3$	−14.1	−12.5	−3.5	−5.6	−4.9	8.4	−5.7
$\Delta\nu_{NO}$	12.1	9.2	−2.3	−6.9	−5.6	1.8	8.3

The vibrational frequencies of HDO, NO, HDO−NO(α), HDO−NO(β), and HDO−NO(β') species are summarized in Table 3.

Finally H_2O-NO, HDO−NO, and D_2O-NO complexes have been irradiated by UV−visible or near-infrared light in order to try to initiate some photoprocesses, but no photochemical reactions were observed.

Theoretical Calculations and Discussion

NO—H_2O. All calculations have been performed with the Gaussian 03 quantum chemical package[18] using the unrestricted wave function with the three parameter hybrid functional of Becke with additional correlation correction by Lee, Young, and Parr (B3LYP),[19,20] For all atoms, the 6-311++G(2d,2p) extended basis set of Pople et al.[21−23] was used.

Calculations of the energetic properties of H_2O-NO complex have already been published by D. W. Ball using the G2 method[6] and by Myszkiewicz et al using the unrestricted MP2, MP4, and CCSD(T) methods.[7] Both studies showed that the most stable geometry for the complex is the one where the bonding occurs between one water hydrogen atom and NO nitrogen atom. The calculations showed that it is a very weak complex with D_e of about 4.5 kJ/mol. The bonding between the H atom of water and the O atom of NO resulted in a less stable structure ($D_e \sim 2$ kJ/mol). Unfortunately the frequencies for the different geometries were not given in the literature.

The B3LYP method was used in order to calculate the frequencies of NO, H_2O, and H_2O-NO species because the MP2 method is unable to determine the vibrational frequency of free and complexed NO. In the case of free NO, the calculated value with MP2 is around 3550 cm^{-1} instead of 1904 cm^{-1} (the experimental value[24]). It is also well-known that this ill-representation does not depend on the basis set.[25] Weakly bound complexes between NO and other molecules have already been investigated with B3LYP,[26,27] which gave satisfactory results.

In the present study, the optimization of the H_2O-NO complex results in five minima given in Figure 9. The two first ones (structures 1 and 2) correspond to complexes where the interaction is between the N atom of NO and the H atom of H_2O. The third structure (3) is the one where NO lies in the plane bisecting the HOH angle (in this case the N atom of NO interacts with the O atom of water). The last two structures (4 and 5) correspond to complexes where the oxygen atom of NO interacts with one H atom of H_2O. The most significant geometrical parameters of the studied complexes and the corresponding binding energies D_e and D_e^{BSSE} are given in Table 4.

One can easily note that, in all the structures, the OH distance of the OH bond interacting with the NO molecule is longer than the one in the free H_2O molecule. The NO distance in structures 1 and 2 is shorter than that of free NO molecule. This fact has already been observed for NO complexes where the NO molecule interacts with another molecule using the N atom.[26,27] When it is the O atom of NO that is responsible for the binding, the NO distance gets longer like in the case of structure 4 and 5. The geometrical parameters for structure 3 are very close to those of free H_2O and NO molecules.

TABLE 7: Calculated Frequency Shifts (cm^{-1}) and Dissociation Energy for the Different Isotopomers of Structure 2 of H_2O-NO

	HOH−NO	DOH−NO	HOD−NO	DOD−NO
$\Delta\nu_1$	−21.5	2.0	−28.1	−14.2
$\Delta\nu_2$	2.5	9.2	−3.9	1.3
$\Delta\nu_3$	−15.7	−39.7	1.8	−12.5
$\Delta\nu_{NO}$	9.2	9.2	9.2	9.2
D_0^{BSSE} (kJ/mol)	0.76	0.94	1.21	1.34

TABLE 8: Comparison of the Calculated Frequency Shifts (cm^{-1}) for Structure 2 of DOH−NO and HOD−NO Complexes and the Experimental Frequency Shifts (cm^{-1}) of HDO−NO(β) and HDO−NO(β') Species

	DOH−NO calcd	HOD−NO calcd	HDO−NO(β') obsd	HDO−NO(β) obsd
$\Delta\nu_1$	2.0	−28.1	7.8	−17.6
$\Delta\nu_2$	9.2	−3.9	12.2	−1.4
$\Delta\nu_3$	−39.7	1.8	−	5.6
$\Delta\nu_{NO}$	9.2	9.2	+8.3	+8.3

The most stable form of the complex is structure 1. Its binding energy of 4.5 kJ/mol is in good agreement with the values reported with other methods.[6,7] However if the binding energy is corrected for BSSE using the Counter Poise method (labeled as D_e^{BSSE}), structure 1 and 2 become isoenergetic with $D_e^{BSSE} =$ 3.6 kJ/mol. The other geometries have smaller binding energies (less than 2.6 kJ/mol). This shows that even if the relative stability of structure 1 and 2 is uncertain, the geometry where N interacts with one H atom of H_2O is more stable than the ones where N interacts with the O atom of H_2O or where O of NO interacts with H of H_2O. Very low value of D_e^{BSSE} indicate that both structure 1 and 2 should be considered as very weak H-bonded or even van der Waals complexes.

The binding energy (corrected for BSSE) of the transition state between structure 1 and structure 2 (where the N−O bond is almost collinear to the O−H bond) was calculated at $D_e^{BSSE} = 2.6$ kJ/mol, showing that a very low barrier height ($\sim$ 1 kJ/mol) for the cis−trans isomerization from structure 1 to structure 2.

The harmonic frequency shifts calculated with the B3LYP method for all the structures of the H_2O-NO complex are listed in Table 5 and compared to experimental shifts for the only detected species NO−$H_2O(\alpha)$ trapped in neon matrix. The comparison between calculated and observed frequency shifts allows us to discard all predicted structures for H_2O-NO complex. Indeed, the analysis of the experimental shifts of the only detected species NO−$H_2O(\alpha)$ trapped in neon matrix shows that OH stretching frequency (ν_1) is red shifted by 4.6 cm^{-1} while the asymmetric stretching (ν_3), the HOH bending (ν_2) and the NO stretching frequencies are both blue shifted by 10.2, 1.5, and 1.7 cm^{-1}, respectively. According to the different calculated structures of H_2O-NO complex, the frequency shifts are not well described by any predicted model. The DFT calculations for NO + H_2O system are not conclusive about the structure of the observed species labeled $H_2O-NO(\alpha)$. The

TABLE 9: Calculated Frequency Shifts (cm^{-1}) for Structure 2 Compared with Experimental Frequency Shifts (cm^{-1}) for HDO−NO(β) HDO−NO(β'), and D_2O−NO(β) Complexes

	HOH−NO calcd	*a* expt	DOH−NO calcd	HDO−NO(β') expt	HOD−NO calcd	HDO−NO(β) expt	DOD−NO calcd	D_2O−NO(β) expt
$\Delta\nu_1$	−21.5	−	2.0	7.8	−28.1	−17.6	−14.2	−9.8
$\Delta\nu_2$	2.5	−	9.2	12.2	−3.9	−1.4	1.3	1.7
$\Delta\nu_3$	−15.7	−	−39.7	−	1.8	5.6	−12.5	−5.7
ν_{NO}	9.2	−	9.2	8.3	9.2	8.3	9.2	8.3

[a] Nonobserved species.

H_2O−NO potential surface was explored systematically at the B3LYP level, but no stable species corresponding to the H_2O−NO(α) species can be calculated. The structure of the observed H_2O−NO(α) complex likely results from columbic attractions between water and nitric oxide, and could be stabilized only in matrix, probably by interaction between NO, water and $(Ne)_n$.

D_2O−NO. The harmonic frequency shifts calculated with the B3LYP method for all the structures of the D_2O−NO complex are listed in Table 6 and compared to the experimental shifts for the two detected species D_2O−NO(α) and D_2O−NO(β). As for H_2O−NO(α) species, no model could reproduce the experimental data for the isotopomer D_2O−NO(α). In the D_2O−NO(β) species case, the comparison between calculated and observed frequency shifts allows us to discard the less stable structures 3, 4, and 5. The experimental frequency shifts are better described with structures 1 and 2 in which OD−N bond is engaged. The values of calculated shifts for structure 1 and 2 are close because of the similar geometries of D_2O−NO complex. The structure 1 and 2 have the same binding energy of 3.6 kJ/mol but when the zero point energy (ZPE) is included, structure 2 is more stable than structure 1 for all isotopes of hydrogen. Thus in the following we will take the structure 2 as a characteristic model of the H_2O−NO complex where bonding occurs between water hydrogen and nitric oxide nitrogen.

HOD—NO and DOH—NO. The calculated shifts and the values of the dissociation energy (D_0^{BSSE}) for the HOH−NO, DOH−NO (interaction between water hydrogen and NO nitrogen), HOD−NO (interaction between water deuterium and NO nitrogen), and DOD−NO complexes for structure 2 are given in Table 7.

Because of their lower ZPE energy, the heavier isotopomers have larger D_0^{BSSE} values. This has already been observed for other water complexes.[28,29] Thus the complex where the interaction is between the deuterium and nitrogen atom is more stable than the one where it is the hydrogen atom that interacts with nitrogen. For structure 2, the energy difference between DOH−NO and HOD−NO complexes is 0.27 kJ/mol. The calculated NO stretching frequency of the complex does not depend on the H/D isotopic substitution. This globally agrees with the experimental observations where upon co-deposition of NO + D_2O or NO + HOD no change of the frequencies of the bands in the NO spectral region was observed.

Calculated (for structure 2) and observed frequency shifts for NO + HOD system are listed in Table 8. The analysis of the shifts show that (as in H_2O−NO(α) and D_2O−NO(α) species case), no model could reproduce the experimental data for HDO−NO(α). The comparison between calculated frequency shifts of DOH−NO and HOD−NO complexes and the observed frequency shifts of NO−HDO(β) and NO−HDO(β') allows us to make a reliable spectral assignment of each species where the predicted DOH−NO and HOD−NO complexes correspond to the observed NO−HDO(β) and NO−HDO(β') species, respectively.

TABLE 10: Comparison of the Calculated Geometric Parameters[a] and Stability of the Most Stable Structures of the H_2O−NO Complex Obtained by B3LYP and CCSD with the 6-311++G(2d,2p) Extended Basis

	structure 1 ($^2A'$)		structure 2 ($^2A'$)		structure 3 ($^2A''$)	
	B3LYP	CCSD	B3LYP	CCSD	B3LYP	CCSD
D_e	4.5	5.3	4.0	4.9	3.5	4.2
D_e^{BSSE}	3.6	3.8	3.6	3.4	2.6	2.6
r_{OH}[b]	0.963	0.957	0.963	0.957	0.961	0.956
r_{OH}	0.961	0.956	0.961	0.956	0.961	0.956
$\angle_{HOH}$	105.2	104.6	105.3	104.7	105.0	104.5
r_{NO}	1.145	1.149	1.146	1.149	1.147	1.15
	r_{H---N}		r_{H---N}		r_{O---N}	
	2.341	2.392	2.356	2.405	2.994	3.124

[a] Distances in Å, angles in degrees, and D_e and D_e^{BSSE} in kJ mol^{-1}. [b] OH bond perturbed by the presence of NO.

This analysis showed that two different types of weakly bound complexes between D_2O and NO could be formed in a neon matrix:

•One species is D_2O−NO(β) which is well described by DFT calculation and in which the OD−N bond is engaged. This species is observed for other D_2O−NO isotopic variant such as the HOD−NO (species labeled β with OD−N bond) and DOH−NO (species labeled $\beta'$with OH−N) complexes, but not for the H_2O−NO isotopomer. No infrared bands of H_2O−NO(β) (complex with an intermolecular OH−N bonding) were observed in our spectra. The calculated and observed frequency shifts of the complex where bonding occurs between water hydrogen and nitric oxide nitrogen are gathered in Table 9. The absence of any signal from HOH−NO complex in our spectra could be explained by the fact that the dissociation energies of DOH−NO, HOD−NO, and DOD−NO are larger than that of HOH−NO.

•The other species D_2O−NO(α) results from Coulombic interactions between NO and D_2O trapped in the neon matrix. The matrix confines the reactants and imposes an unstable geometry which could not be determined by any theoretical model. This unstable species is probably stabilized in the solid cage, probably by the guest−host interactions. This species is observed for all D_2O−NO(α) isotopomers (H_2O−NO(α) and HOD−NO(α)).

The dissociation energy (D_0^{BSSE}) of the nitric oxide water complex, in which the water hydrogen and the NO nitrogen are weakly bounded, is predicted on the order of 1 kJ/mol. The frequency shifts with respect to the monomeric moieties are weak but they are slightly higher than those measured with the second 1:1 H_2O−NO species which is observed only in experiment. The comparison between the frequency shifts of the two H_2O−NO complexes suggests that the binding energy for the H_2O−NO species in which NO is connected to H_2O by Coulombic attractions, is even lower than 1 kJ/mol.

Finally, to support the theoretical results obtained with DFT/B3LYP, we have performed some additional calculations at a higher level, CCSD approach using the 6-311++G(2d,2p) basis set. The comparison between the two theoretical studies for the most stable structures of H_2O-NO complexes is gathered in Table 10. One can note that the DFT results are very similar to the CCSD ones, indicating the reliability of our theoretical description done with DFT method in this study.

Conclusion

The IR spectra of NO + H_2O, NO + HDO, and NO + D_2O isolated in solid neon at low temperature have been investigated. On the basis of a comparison between the infrared spectra and the results of DFT calculations, two different weakly bounded complexes between water and nitric oxide can be formed in matrix. The first species is a 1:1 H_2O-NO complex in which O−H−N (and OD−N) intermolecular bonds are engaged. For this complex only DOD−NO, HOD−NO, and DOH−NO isotopic species have been detected experimentally. No IR bands of HOH−NO were observed in our spectra. A plausible reason is that the dissociation energy of HOH−NO (D_0 = 0.76 kJ/mol) is lower than those of DOD−NO (D_0 = 1.34 kJ/mol), HOD−NO (D_0 = 1.21 kJ/mol), and DOH−NO (D_0 = 0.94 kJ/mol). The energy values for DOD−NO and HOD−NO are close to each other since NO nitrogen is connected to the D atom rather than to H atom. The same remark could be done for the energy values for HOH−NO and DOH−NO. For the second detected 1:1 H_2O-NO complex and its isotopic variants, the potential surface was explored systematically at the B3LYP level but no stable species corresponding to the complex could be calculated. The structure of the second observed 1:1 H_2O-NO complex results from columbic attractions between water and nitric oxide and could be stabilized only in the matrix, probably by interaction between NO, H_2O, and $(Ne)_n$.

References and Notes

(1) Sandler, P.; Jung, J. O.; Szczesniak, M. M.; Buch, V. *J. Chem. Phys* **1994**, *101*, 1378. Dennis, C. R.; Whitham, C. J.; Low, R. J.; Howard, B. J. *Chem. Phys. Lett.* **1998**, *282*, 421. Klos, J.; Chalasinski, G.; Berry, M. T.; Bukowski, R.; Cybulski, S. M. *J. Chem. Phys.* **2000**, *112*, 2195.

(2) Coussan, S.; Loutellier, A.; Perchard, J. P.; Racine, S.; Bouteiller, Y. *J. Mol. Struct.* **1998,** *471*, 37.

(3) Hirabayashi, S.; Ohno, K.; Abe, H.; Yamada, K. M. T. *J. Chem. Phys.* **2005,** 122.

(4) Kjaergaard, H. G.; Low, G. R.; Robinson, T. W.; Howard, D. L. *J. Phys. Chem. A* **2002**, *106*, 8955.

(5) Cooper, P. D.; Kjaergaard, H. G.; Langford, V. S.; Mckinley, A. J.; Quickenden, T. I.; Robinson, T. W.; Schofield, D. P. *J. Phys. Chem. A* **2005**, *109*, 4274.

(6) Ball, D. W. *J. Phys. Chem. A* **1997**, *101*, 4835.

(7) Myszkiewicz, G.; Sadlej, J. *Chem. Phys. Lett.* **2000**, *318*, 232.

(8) Fredin, L. *Chem. Scr.* **1973**, *4*, 97.

(9) Givan, A.; Loewenechuss, A.; Nielsen, C. J. *PCCP* **1999**, *1*, 37.

(10) Danset, D.; Manceron, L. *J. Phys. Chem. A* **2003**, *107*, 11324.

(11) Kometer, R.; Legay, F.; Legay-Sommaire, N.; Schwentner, N. *J. Chem. Phys.* **1994**, *100*, 8737.

(12) Perchard, J. P. *Chem. Phys*. **2001**, *273*, 217.

(13) Engdahl, A.; Nelander, B. *J. Chem. Phys.* **1989**, *91*, 6604.

(14) Michaut, X.; Vasserot, A. M.; Abouaf, M. L. *Vib. Spectrosc.* **2004**, *34*, 83.

(15) Forney, D.; Jacox, M. E.; Thompson, W. E. *J. Mol. Struct.* **1993**, *157*, 479.

(16) Knözinger, E.; Wittenbeck, R. *J. Am. Chem. Soc.* **1983**, *105*, 2154.

(17) Dozova, N.; Krim, L.; Alikhani, M. E.; Lacome, N. *J. Phys. Chem. A* **2005**, *109*, 10273.

(18) Frisch, M. J.; Trucks, G. W.; Schlegel, H. B.; et al. Gaussian 03, Revision B.02; Gaussian, Inc.: Pittsburgh, PA, 2003.

(19) Becke, A. D. *J. Chem. Phys*. **1993**, *98*, 5648.

(20) Lee, C.; Young, E.; Parr, R. G. *Phys. Rev. B* **1988**, *37*, 785.

(21) Krishnan, R.; Binkley, J. S.; Seeger, R.; Pople, J. A. *J. Chem. Phys.* **1980**, *72*, 650.

(22) Clark, T.; Chandrasekhar, J.; Spitznagel, G. W.; R. Schleyer, P. V. *J. Comput. Chem.* **1983**, *4*, 294.

(23) Frisch, M. J.; Pople, J. A.; Binkley, J. S. *J. Chem. Phys.* **1984**, *80*, 3265.

(24) Huber, K. P.; Herzberg, G. *Molecular Spectra and Molecular Structure Constant of Diatomic Molecules*; van Nostrand Reinhold: New York, 1979.

(25) NIST Computational Chemistry Comparison and Benchmark Database, NIST Standard Reference Database Number 101, Release 12, Aug 2005, Johnson, Russell D., III, Ed.; http://srdata.nist.gov/cccbdb.

(26) Zhou, M.; Zhang, L.; Qin, Q. *J. Am. Chem. Soc.* **2000**, *122*, 4483.

(27) Krim, L.; Alikhani, E. *Chem. Phys*. **1998**, *237*, 265.

(28) Engdahl, A.; Nelander, B. *J. Chem. Phys.* **1989**, *91*, 6604.

(29) Futami, Y.; Kudoh, S.; Takayanagi, M.; Nakata, M. *Chem. Phys. Lett.* **2002**, *357*, 209.